

# Ultraviolet light induced changes in polyimide liquid-crystal alignment films

J. Lu, S. V. Deshpande, E. Gulari, and J. Kanicki<sup>a)</sup>

Center for Display Technology and Manufacturing, The University of Michigan, Ann Arbor, Michigan 48109

W. L. Warren

Advanced Materials Laboratory, Sandia National Laboratories, Albuquerque, New Mexico 87185-1349

(Received 20 October 1995; accepted for publication 25 July 1996)

Ultraviolet light induced changes in polyimide liquid-crystal alignment films were investigated. Infrared, UV-visible, x-ray photoelectron spectroscopy, and electron-spin-resonance measurements indicated that bond breaking and subsequent oxidation reactions occur in polyimide films (SE7210, OCG284, DuPont 2555 and 2540) during the broadband UV illumination in air. Mechanical rubbing has no effect on the optical and magnetic properties but it causes the removal of the UV-exposed film. Capacitance-voltage measurements indicate that there is a slight decrease in dielectric constant and creation of net negative charges in the film after UV exposure. Surface tension of polyimide films before and after UV illumination and changes in the pretilt angle of the polyimide surface following UV exposure have also been studied. The decrease in pretilt angle following UV illumination is attributed to an increase in surface tension. Our results indicate that a simple UV technique can be used to achieve domain divided liquid-crystal pixel electrode design with improved viewing characteristics. © 1996 American Institute of Physics. [S0021-8979(96)02021-X]

## I. INTRODUCTION

Active matrix liquid-crystal displays (AMLCDs) offer the best image quality and display performance among various kinds of liquid-crystal displays [twisted nematic (TN), supertwisted nematic, ferroelectric, polymer dispersed]; however, the narrow and nonuniform viewing angle characteristics, and consequently gray-scale errors, could limit the display applications. This limitation prevents rapid advances in the active matrix TN-LCD technology. Today it is increasingly believed that the display properties, to a large extent, depend on the alignment layers of liquid crystal. To solve this angular dependence problem, multidomain LCDs<sup>1-4</sup> and random domain alignment<sup>5</sup> have been proposed. The multirubbing technique to achieve two-domain TN-LCD is very complicated and an uneconomical process.<sup>1</sup> Using a special photomask with subsequent UV curing of photoanisotropic alignment layer to form quartered subpixel was proposed by Hashimoto *et al.*;<sup>3</sup> however, it was observed that the linearly polymerized poly-(vinyl cinnamate) produces very low<sup>3</sup> and unstable pretilt angle,<sup>6</sup> which is not suitable in AMLCD. The random domain alignment, proposed by Limura *et al.*<sup>5</sup> using a nonrubbing technique, produces a display in which each pixel consists of several hundreds of domains. With this approach, wide and uniform viewing angle characteristics are obtained, but the contrast ratio is severely compromised. In other recent studies,<sup>7,8</sup> polarized UV light has been used to treat polyimide (PI) layers to obtain liquid-crystal alignment. These studies have demonstrated that dual-domain twisted nematic (DDTN) cells may be fabricated by a combination of polarized-UV and multirubbing technique. Improved viewing angle characteristics were obtained without compromising the contrast ratio.<sup>7</sup>

It is well documented that exposure of polymers to UV radiation can lead to extensive physical and chemical modification of polymeric materials.<sup>9</sup> These changes in properties may have both detrimental and beneficial consequences in determining the end use of the polymer. Recently, the IBM group has reported an application of the UV-induced changes in pretilt angle for fabrication of two-domain liquid-crystal displays.<sup>10</sup> We also find that the pretilt angle of PI alignment layers can be altered by UV illumination and the decrease in pretilt angle following UV illumination is attributed to an increase in surface tension.<sup>11</sup> In this article the effect of broadband UV induced changes on both rubbed and nonrubbed PI films are described.

## II. EXPERIMENTAL PROCEDURE

Four different PIs were used in this study: Nissan SE 7210, DuPont PI 2555, DuPont PI 2540, and OCG 284 (see Fig. 1). Nissan SE 7210, PI 2555, PI 2540 are in the form of polyamic acid solutions while OCG 284 is a preimidized PI. The PIs were spin coated on to silicon wafers and quartz substrates. The films were then dried on a hot plate at 80 °C for 10 min followed by a final cure for 1 h in an oven under nitrogen purge. The final curing was done at 300, 270, 300, and 250 °C for Nissan SE 7210, DuPont PI 2555, DuPont PI 2540, and OCG 284, respectively, in order to obtain fully imidized polymer film. The resulting films were exposed to broadband UV illumination. A mercury lamp (200 W) was used in these studies with an average power density of 4.45 mW/cm<sup>2</sup>. The power meter used for this measurement was from Murmir Corporation, peaked for 405 nm line of a Hg lamp.

The film thickness was measured by a surface profilometer and ellipsometry. A number of techniques was used to characterize the UV-exposed and unexposed films including:

<sup>a)</sup>Author to whom correspondence should be addressed.

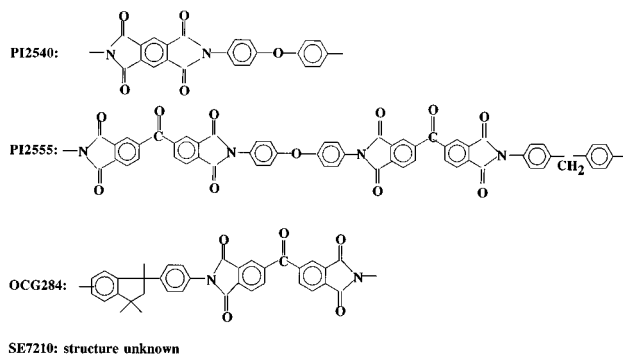


FIG. 1. Chemical structure of the polyimides.

infrared [Fourier transform infrared (FTIR)] spectroscopy, x-ray photoelectron spectroscopy (XPS), electron spin resonance (ESR), 1.0 MHz capacitance–voltage ( $C-V$ ) measurements, and surface tension measurements. The FTIR measurements were done with a BioRad FTS-40 spectrometer. The films were coated on silicon wafers for FTIR measurements. XPS was performed with a Perkin–Elmer system. The ESR measurements were made on an X-band spectrometer using the  $TE_{104}$  or an optical access microwave cavity at 25 K for two different power levels. The films were illuminated *in situ* and/or *ex situ* with a broadband light from a 100 W Hg-arc Oriol lamp. Defect densities were derived by comparing the double numerical integral of the measured derivative power absorption spectrum with that of a calibrated weak pitch standard. The effect of mechanical rubbing on the PI film thickness after exposure to UV was also studied. Liquid-crystal cells used in this experiment consisted of two antiparallel rubbed polymer films coated on indium–tin–oxide glass plates. The SE 7210 films, cured at 180 °C for 1 h in an oven under nitrogen purge, were used for pretilt angle studies. The pretilt angle was measured by the crystal rotation method.<sup>12</sup> The liquid crystal used for filling the cells was ZLI-5080 from E. Merck & Company.

### III. EXPERIMENTAL RESULTS

#### A. Spectroscopic analysis

Spectroscopic methods can be used as an analytical tool to probe structure and to obtain information on physico-chemical changes of polymeric materials upon radiation. The advantages of spectroscopic measurements over other means of polymer characterization are that they are nondestructive and are a rapid means of providing information at molecular level.

##### 1. Infrared spectroscopy

It was found that all polymers absorb UV light and bond-breaking reactions occurred in all of these polymers after exposure to broadband UV light. Figure 2(a) shows the infrared spectrum of the unexposed Nissan SE 7210 film after curing at 300 °C for 1 h. The characteristic absorption peaks associated with C–O–C ( $1237\text{ cm}^{-1}$ ), imide group ( $1387$  and  $1718\text{ cm}^{-1}$ ), and the aromatic ring ( $1501$  and  $724\text{ cm}^{-1}$ ) appear in the spectrum. The UV-illuminated spectrum is shown in Fig. 2(b) and the difference spectrum between

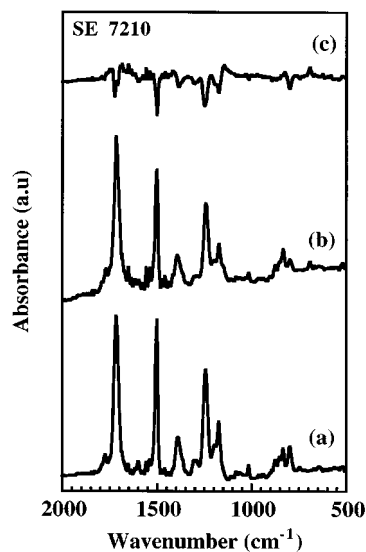


FIG. 2. FTIR spectra of SE 7210; (a) before UV illumination; (b) after UV illumination; and (c) difference of after and before UV illumination.

the UV-exposed PI film and the unexposed is shown in Fig. 2(c). This figure shows that following UV illumination the intensities of most of the peaks decrease. Careful analysis of the FTIR spectra shows that the intensity of the peak at  $1715\text{ cm}^{-1}$ , which can be associated with the  $>C=O$  group, initially decreases with illumination time and then increases. This final increase could be associated with oxidation of the polymer fragments. These results indicate that bond-breaking reactions (with subsequent oxidation) occur in polymer films after UV exposure. The intermolecular or intramolecular migration of reactive radicals from the UV-sensitive groups may cause all the bonds to break in the polymer and polymer chain may provide a pathway for the migration and trapping of reaction species.<sup>13</sup>

Although the deposition of UV photons is spatially random on the molecular scale, the chemical changes are not random. The selectivity of chemical change can be correlated with the sensitivity of some chemical groups to radiation and the resistance of others. The degree of chemical reactions in irradiated polymers are dependent on physical as well as chemical factors.<sup>13</sup> Four different kinds of fully imidized polyimides were exposed to broadband UV light. Figure 3 shows the percentage change of peak intensity of the C–N stretching mode after UV exposure as a function of total illumination energy incident on various polyimide samples. The same trend was also observed for peaks at 1173, 1240, and  $1500\text{ cm}^{-1}$  corresponding to  $-\text{CH}$ , C–O–C, and C=C bonds, respectively. OCG 284 is more UV sensitive than PI 2555 and PI 2540 because of the presence of the dimethyl-cyclopentane group. Furthermore, PI 2540 is partially crystalline while PI 2555 is amorphous. Bond breaking occurs in polymer molecules in the solid state to form two free radicals and the limited mobility of the resultant chain fragments prevents permanent scission.<sup>14</sup> Therefore, the scission yield is higher in amorphous PI 2555 polymer compared with crystalline PI 2540 polymer. Among all the poly-

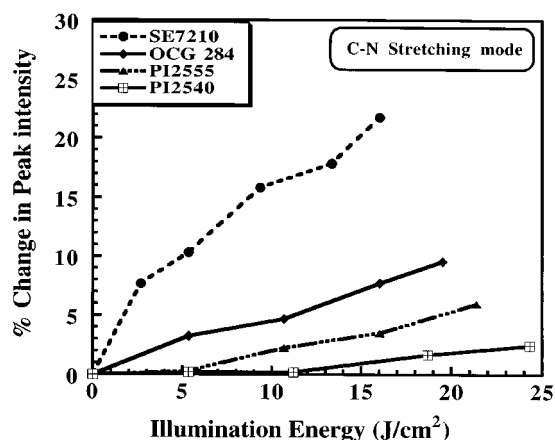


FIG. 3. The change in peak intensity of the C-N stretching mode after UV illumination for different polyimides.

mers we studied, SE 7210 is the most susceptible to UV radiation. It is expected that there is a lesser degree of aromaticity and crystallinity in this polymer. SE 7210 was chosen for conducting further analysis with the purpose of revealing the effect of UV light on polyimide alignment films. The sensitivity toward UV illumination for varying degrees of imidation was also investigated and is shown in Fig. 4. Based on the same argument, the lower imidation polymer would contain more UV sensitive groups ( $>N-H$ ,  $HO-C=O$ ) and, therefore, is more UV sensitive.

## 2. UV-visible spectroscopy

UV spectra of molecules are associated with the electronic transitions involving  $\pi$  and/or  $n$  electron systems. Polyimides containing aromatic and carbonyl groups have particularly strong absorption in the UV regions. In this study we have also observed the large changes in UV-visible spectra of polyimides induced by broadband UV illumination. Figure 5 shows the changes in the absorption spectra of SE 7210 following UV exposure. The illuminated SE 7210 polyimide absorbed more low-energy photons than the unilluminated sample and the difference of absorption coefficient  $\Delta\alpha$ , defined at 330 nm, increased with the illumination time, as shown in Fig. 5. The changes in the subband absorption for PI 2555 and OCG 284 were very small ( $<5\%$ ) and were below the detection limit of our UV-visible spectrometer. These small changes for PI 2555 were detected by the more sensitive technique of ESR, as discussed in the following subsection. Since the UV-visible absorption is sensitive to the chemical structure, polymer conformation, and molecular environment, the change in spectra by broadband UV can be related to the changes in the chemical structure and molecular environment.<sup>15,16</sup> The continuous decrease of absorption in the range 5.8–6.5 eV, after UV illumination, clearly indicates that breakage of the aromatic ring and creation of radicals has taken place. This decrease in absorption as a function of increasing UV-illumination time was consistently observed for all the polymers. At the same time an increase in subband-gap absorption was observed. This increase can be directly correlated with an increase in ESR signal, as discussed below. Therefore, the creation of radicals could be associated with the increase in subband-gap absorption. Also, the optical band gap  $E_g^{04}$ , defined at  $\alpha=10^4 \text{ cm}^{-1}$ , changes after UV illumination.  $E_g^{04}$  decreases with illumination time, which is consistent with the bond-breakage phenomenon described above.

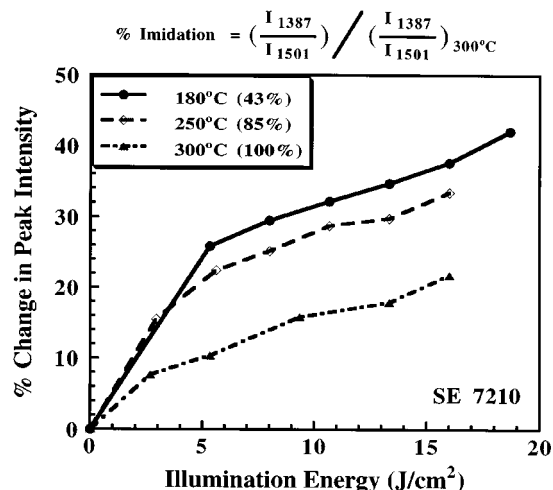


FIG. 4. Effect of percent imidation on the UV sensitivity for SE 7210.

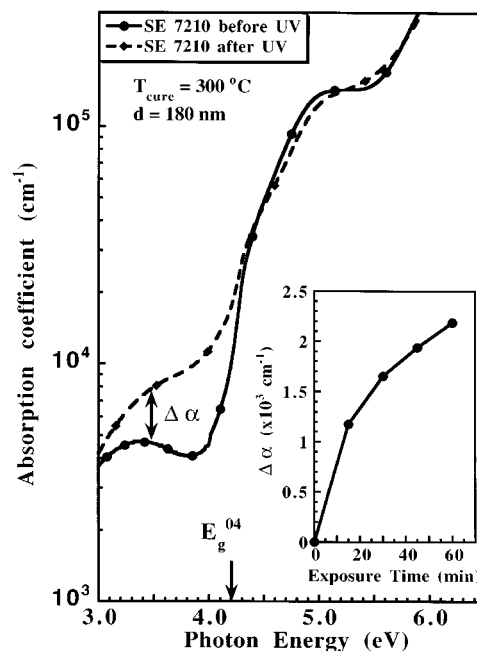


FIG. 5. The changes in the UV-visible absorption spectra for SE 7210. The change in absorption coefficient as a function of exposure time is shown in the inset.

luminated sample and the difference of absorption coefficient  $\Delta\alpha$ , defined at 330 nm, increased with the illumination time, as shown in Fig. 5. The changes in the subband absorption for PI 2555 and OCG 284 were very small ( $<5\%$ ) and were below the detection limit of our UV-visible spectrometer. These small changes for PI 2555 were detected by the more sensitive technique of ESR, as discussed in the following subsection. Since the UV-visible absorption is sensitive to the chemical structure, polymer conformation, and molecular environment, the change in spectra by broadband UV can be related to the changes in the chemical structure and molecular environment.<sup>15,16</sup> The continuous decrease of absorption in the range 5.8–6.5 eV, after UV illumination, clearly indicates that breakage of the aromatic ring and creation of radicals has taken place. This decrease in absorption as a function of increasing UV-illumination time was consistently observed for all the polymers. At the same time an increase in subband-gap absorption was observed. This increase can be directly correlated with an increase in ESR signal, as discussed below. Therefore, the creation of radicals could be associated with the increase in subband-gap absorption. Also, the optical band gap  $E_g^{04}$ , defined at  $\alpha=10^4 \text{ cm}^{-1}$ , changes after UV illumination.  $E_g^{04}$  decreases with illumination time, which is consistent with the bond-breakage phenomenon described above.

## 3. Electron spin resonance (ESR)

The photoinduced bond breaking has been further supported by an ESR experiment. There are a few free radicals in the unirradiated sample, but the ESR signal intensity was greatly enhanced as a result of UV exposure due to formation of free radicals. For example, SE 7210 PI exposed to broadband UV radiation gives an ESR spectrum, as depicted in

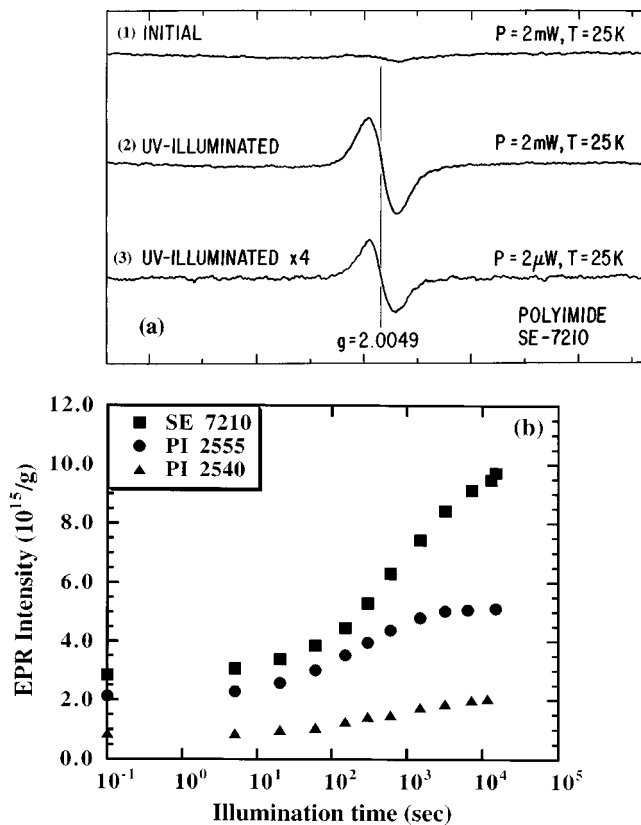


FIG. 6. Changes in spin density as measured by electron spin resonance: (a) ESR spectra of SE 7210 (1) before UV illumination, (2) and (3) after UV illumination at different microwave power levels; (b) increase in spin density for different polyimides.

Fig. 6(a). We have found that the spin intensity in PI SE 7210 increased from  $1.5 \times 10^{17}$  to  $2 \times 10^{18} \text{ cm}^{-3}$  after UV illumination. In both unilluminated and UV-illuminated films only one isotropic signal (with  $g = 2.0049$ ) was observed at 25 K and two different microwave powers. The experiment was done at two different power levels to look for any additional peaks in the ESR spectrum. According to the  $g$  value, the ESR signal may be associated with the alkoxy- and/or alkyl-type radicals but not with peroxide radicals.<sup>17</sup> Furthermore, mechanical rubbing has no effect on the spin intensity in the PI both before and after UV exposure.

The dependence of spin density on illumination time for various PIs is shown in Fig. 6(b). For these measurements, powder samples of these PIs were prepared by removing films deposited on silicon wafers. As shown in this figure, the spin density for SE 7210 increases with the dose of UV illumination. The other polymers (PI 2555 and PI 2540) also show a similar trend with smaller changes. The result is consistent with the changes in the UV-visible spectra of SE 7210, i.e., both the number of point defects, represented by unpaired electrons, and subband-gap absorption increase with illumination time. Thus, the ESR and subband-gap absorption could be associated with the same radical. The ESR result is also consistent with FTIR data indicating that SE 7210 PI is more UV sensitive than the other three polymers films. Therefore, SE 7210 must contain aromatic and aliphatic (cyclobutane) rings. The presence of aliphatic ring is

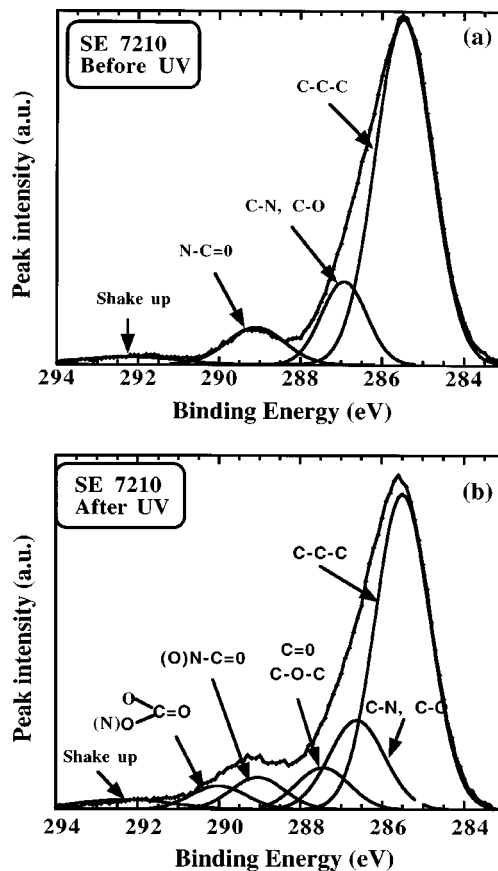


FIG. 7. XPS Spectra of SE 7210: (a) before and (b) after UV illumination.

supported by the presence of two absorption peaks in the  $2900 \text{ cm}^{-1}$  region of the FTIR spectrum (not shown in Fig. 2). The chemical structure of SE 7210 is considered to be a Nissan trade secret.

#### 4. X-ray photoelectron spectroscopy (XPS)

The changes in the surface composition of PI films after UV-exposure have been determined by XPS. In all the PIs studied here, we observed increased levels of oxygen on the surface. This was accompanied by an increase in the contribution of  $>\text{C}=\text{O}$ ,  $-\text{COOH}$ , and  $-\text{O}-\text{C}-\text{O}-$  groups to the carbon ( $1s$ ) and oxygen ( $1s$ ) peaks in the spectra. This indicates that after the UV-induced bond breaking, the free radicals that are generated tend to stabilize by oxidation.<sup>17-19</sup> The changes in the carbon ( $1s$ ) peak due to UV exposure are shown in Fig. 7 for the SE 7210 sample. The decrease in intensity of the peaks at 285.0 and 292.0 eV indicated a loss of aromaticity or breakage of the benzene ring. There was also an increase in peak intensity of the  $-\text{C}-\text{O}-\text{C}-$  feature and two new oxygenated carbon components appeared at 287.5 and 290.0 eV as a result of oxidation. The results of XPS analysis are summarized in Table I. For this sample the atomic oxygen composition increased from 12.5% to 19.0% after 80 min of exposure to  $4.45 \text{ mW}/\text{cm}^2$  of broadband UV illumination. The surface atomic composition of SE 7210 remains the same after the removal top layers (40 nm) of film by ultrasonic treatment. This also indicates that the UV-

TABLE I. Surface atomic composition of SE 7210 polyimide as measured by XPS.

Sample treatment <sup>a</sup>	O 1s (%)	N 1s (%)	C 1s (%)
Unexposed	12.83	4.90	82.47
UV exposed for 60 min	17.34	5.05	77.61
UV exposed for 80 min	19.01	4.85	76.13
UV exposed for 80 min and After ultrasonic treatment for 2 h	19.40	4.54	76.06

<sup>a</sup>All samples were cured for 1.0 h at 180 °C.

induced photoreaction is a bulk rather than a surface effect. The other polymers also showed similar surface composition changes indicating that oxidation occurred following UV illumination.

### B. Effect of mechanical rubbing

Due to oxidation in the UV-exposed film, it would be expected that the film would become brittle and will form a powderlike debris after mechanical rubbing. Indeed, we have observed that mechanical rubbing of the UV-exposed SE 7210 polyimide film causes film removal, as much as 120 nm depending on the rubbing strength. The powderlike debris formed due to rubbing could be brushed away by the rubbing cloth. Within the investigated rubbing strength between 179 and 696 nm, the change in the film thickness is directly related to the rubbing strength as shown in Fig. 8. Also the film removal is independent of film thickness indicating that the effect of UV light is bulk rather than surface-effect and as expected the UV-exposed film is mechanically less stable. Finally, the reduction in thickness for a given rubbing strength will depend on UV-light energy;  $\Delta d$  will be larger for higher UV energies. We adopted the following equation<sup>20</sup> for determining the rubbing strength (RS):

$$RS = NM[(2\pi rn/v) + 1], \quad (1)$$

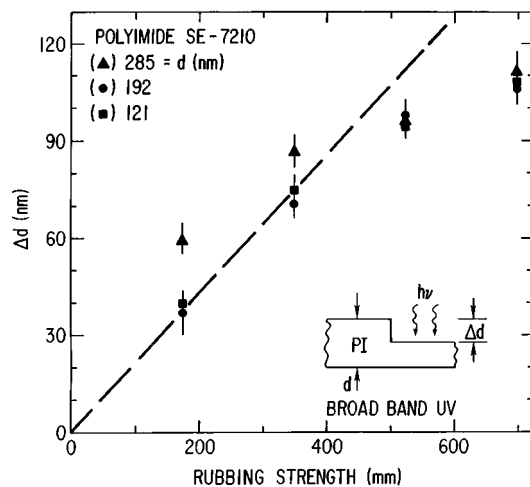


FIG. 8. The change of film thickness vs the rubbing strength for SE 7210. The dotted line has been drawn to guide the eye. The schematic in the inset represents the change  $\Delta d$  in thickness due to film removal after rubbing subsequent to UV exposure. This figure was adopted from Ref. 11.

where  $N$  is the number of the repeated times of rubbing,  $M$  is the depth of the deformed fibers of the cloth due to the pressed contact (1.6 mm),  $n$  is the rotation rate of the drum (200 rpm),  $v$  is the translating speed of the substrate (24 mm/s), and  $r$  is the radius of the drum (76.2 mm).

Similar results were obtained when the UV-exposed films were subjected to few minutes of ultrasonic agitation. The top layers (40 nm) of the films could be removed indicating that the top layers of the UV-exposed films were mechanically less stable. Furthermore, we have also observed for SE 7210 that the thickness of the film removed decreases with increasing imidation temperature. This indicates that as the imidation temperature (or % imidation) is increased the PI becomes less susceptible to UV light, which is consistent with the FTIR data shown in Fig. 5.

### C. Capacitance–Voltage ( $C-V$ ) measurements

It is expected that the combination of bond breaking and film oxidation would produce an excess charge inside and/or at the PI surface. We have used the Al/PI/thermal oxide (200 Å)/ $p$ -type  $c$ -Si (111) structure to investigate the UV-induced space-charge formation through the analysis of high-frequency (1 MHz) capacitance–voltage characteristics. The device is positioned on a probe station and is connected to a  $C-V$  bridge. The bridge superimposes a small ac (25 mV) signal on top of the preselected dc voltage and monitors the resulting ac current flowing into the test dot. The test dot was 2.0 mm in diameter. An example of a  $C-V$  curve for SE 7210 is shown in Fig. 9(a). It should be noted that there was no detectable change in the film thickness before and after 60 min of UV illumination. Thus, the decrease in the maximum capacitance is likely associated with the decrease in the polyimide dielectric constant from  $\epsilon=3.0$  (before UV exposure) to  $\epsilon=2.7$  (after UV exposure). This result is confirmed by a decrease in film refractive index as measured by ellipsometry. The minimum capacitance does not change after UV exposure indicating that the  $c$ -Si substrate is not affected by UV light. Also, 200-Å-thick thermal oxide is not affected by UV-light in this experiment. A slight shift in  $C-V$  curves toward more negative voltages (photocreation of positive charges) can be observed for thicker thermal oxide layers. In our experiment, the shift of  $C-V$  curves towards less negative biases indicates that either negative charges accumulate in the PI layer after UV-exposure or existing positive charges are annihilated due to photogenerated electrons. This shift is represented by  $\Delta V$ , which is defined as the voltage shift at the average capacitance for the measurement, i.e.,  $(C_{\max} + C_{\min})/2$ .

The distribution of photoinduced charges in the polyimide layer was verified by performing  $C-V$  measurements for polyimide films of different thicknesses, and the results are shown in Fig. 9(b). As shown in this plot, the slope of  $\log(\Delta V)$  vs  $\log(\text{film thickness})$  is close to 2.0. This indicates that the net negative charges generated in the PI film after UV exposure are distributed uniformly in the bulk of the film. Based on this observation, we can calculate the UV-induced density of negative charge  $N_{\text{eff}}$  using the following equation:

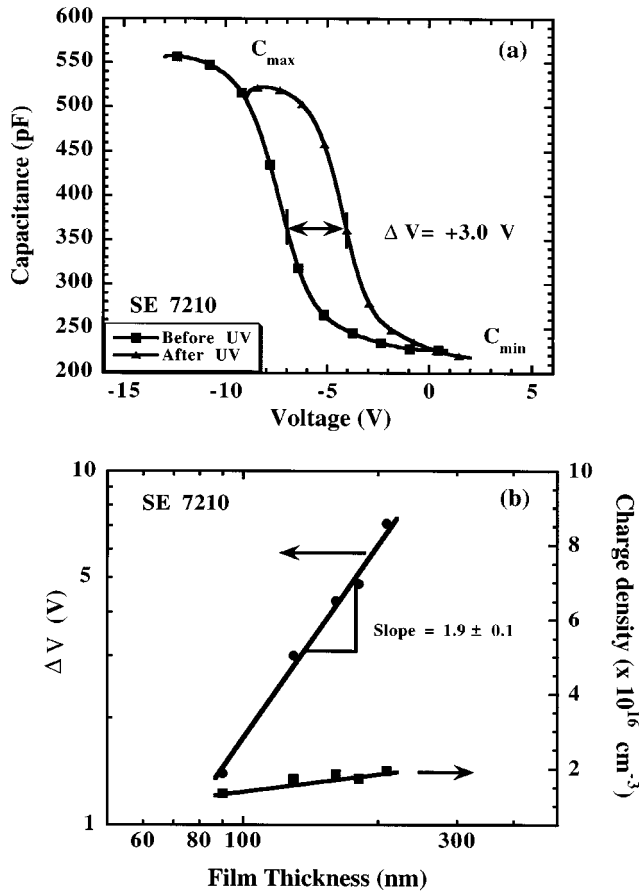


FIG. 9. Results of  $C$ - $V$  measurements on SE 7210 polyimide; (a) UV-induced shift in the  $C$ - $V$  curve for a 130.0-nm-thick film, and (b) change in the voltage  $\Delta V$  for various polyimide film thicknesses.

$$N_{\text{eff}} = [C_{\text{max}}(\Delta V)] / (qV), \quad (2)$$

where  $C_{\text{max}}$  is the maximum capacitance,  $q$  is the electronic charge ( $1.602 \times 10^{-19}$  C), and  $V$  is the test volume (area of the dot  $\times$  film thickness) of the polyimide. A value of  $N_{\text{eff}}$  on the order of  $2.0 \times 10^{16} \text{ cm}^{-3}$  was obtained for SE 7210 after broadband UV illumination. This light-induced charge will not only modify the LC-PI interaction but can also enhance the dc offset voltage generated in a LC alignment cell.<sup>21,22</sup> It is known that such a dc voltage can be generated in a LC cell which has different front and rear alignment layers.<sup>21</sup> Furthermore, the trapping sites generated during UV illumination could trap the carriers during ac voltage operation of the display and generate an additional dc offset voltage shift.

#### D. Surface tension and pretilt angle measurements

The bulk and surface charges induced by UV light (as observed in  $C$ - $V$  studies) are expected to affect the interaction between PI and the liquid crystal. The pretilt angle between LC and alignment layer depends on the physical and chemical properties of alignment layer surface,<sup>23,24</sup> thus, the control of pretilt angle can be achieved by the control of surface tension.<sup>25,26</sup> It is expected that both the surface tension and pretilt angle would be modified by UV illumination.

TABLE II. Surface tension of SE 7210 polyimide films subjected to various conditions.

Sample treatment <sup>a</sup>	Imidation ratio (%)	Surface tension (dyn/cm)	Pretilt angle (deg)
Cured at 180 °C	43	36–37	5.9
Cured at 180 °C (and UV exposed for 60 min)	43	43–45	1.2
Cured at 250 °C	85	41–43	5.4
Cured at 300 °C	100	42–44	5.1

<sup>a</sup>All samples were cured for 1.0 h at the temperatures mentioned in the table and illuminated with UV light of 5.0 mW/cm<sup>2</sup>.

We have, therefore, measured the surface tension of the PI films before and after UV illumination and also as a function of the curing temperature of the PI.

Surface tension consists of dispersion component  $\gamma_{\text{polymer}}^d$  and polar component  $\gamma_{\text{polymer}}^p$ , which were estimated from the contact angles  $\theta$  of water and glycerol on polymer samples using the following equation:<sup>26</sup>

$$1 + \cos \theta = \frac{1}{\gamma_{\text{water}}} \left( \frac{4 \gamma_{\text{polymer}}^d \gamma_{\text{water}}^d}{\gamma_{\text{polymer}}^d + \gamma_{\text{water}}^d} + \frac{4 \gamma_{\text{polymer}}^p \gamma_{\text{water}}^p}{\gamma_{\text{polymer}}^p + \gamma_{\text{water}}^p} \right),$$

$$1 + \cos \theta = \frac{1}{\gamma_{\text{glycerol}}} \left( \frac{4 \gamma_{\text{polymer}}^d \gamma_{\text{glycerol}}^d}{\gamma_{\text{polymer}}^d + \gamma_{\text{glycerol}}^d} + \frac{4 \gamma_{\text{polymer}}^p \gamma_{\text{glycerol}}^p}{\gamma_{\text{polymer}}^p + \gamma_{\text{glycerol}}^p} \right), \quad (3)$$

$$\gamma_{\text{polymer}} = \gamma_{\text{polymer}}^d + \gamma_{\text{polymer}}^p,$$

where  $\gamma_{\text{water}}^d = 22$  dyn/cm,  $\gamma_{\text{water}}^p = 52$  dyn/cm,  $\gamma_{\text{glycerol}}^d = 34$  dyn/cm, and  $\gamma_{\text{glycerol}}^p = 33$  dyn/cm.

The two unknowns, namely, the dispersion  $\gamma_{\text{polymer}}^d$  and polar  $\gamma_{\text{polymer}}^p$  components, were calculated by simultaneously solving the above two equations. As shown in Table II, the surface tension  $\gamma_{\text{polymer}}$  increased after UV illumination and the same effect can be achieved by a higher degree of imidation. Since the surface tension of UV-modified PI films has changed, it is expected that the interaction between liquid crystal and PI alignment films will also be altered.

The pretilt angle of the rubbed PI was determined by the crystal rotation method. As shown in Table II, the pretilt angle continuously decreased with increasing UV-illumination time. It should be noted that high dosage of UV light is not recommended since the pretilt angle is too small and the LC alignment is not good. Furthermore, the decrease in pretilt angle is strongly correlated to the increase in surface tension of the UV-exposed surfaces, as reported elsewhere.<sup>27</sup>

#### IV. DISCUSSION

The effect of UV light on the pretilt angle of PI alignment layers could be utilized to obtain multidomain LC displays. The use of multiple domains, with different pretilt angles, within a pixel could provide wider viewing angle characteristics for AMLC displays.<sup>7,10,28,29</sup> Such a display

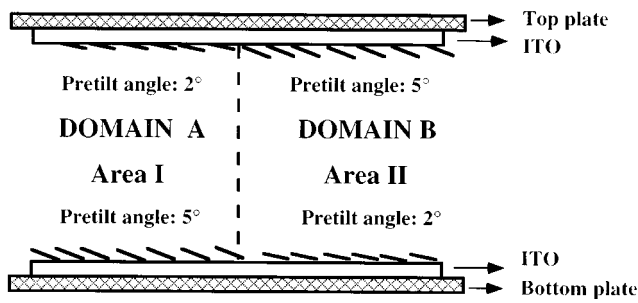


FIG. 10. Cross section of the proposed two-domain TN-LCD structure using a UV-photomask two-domain technique.

could be easily and reliably fabricated using a photomask to change the pretilt angle of the desired area within the pixel. An example of a two-domain twisted nematic (TDTN) cell is shown in Figure 10. In this example, the PI is first spin coated on to the lower plate and then rubbed in the appropriate direction. Area II is then selectively exposed to UV light (using a photomask) in order to decrease the pretilt angle to a desired value. This simple procedure can produce two domains on each LC pixel on the lower glass plate. The same procedure can be applied for the top glass plate. This approach is easy to implement in manufacturing since it requires only two additional steps of UV exposure, prior to PI rubbing. It is much simpler than the multirubbing<sup>1,7</sup> approach as it does not require additional photoresist processing. However, in this process the PI on the top and bottom plates are modified and this can produce a large dc offset voltage during the ac voltage operation of the AMLCD.<sup>22</sup> If this dc offset exceeds certain limits, it can introduce an image-sticking problem and produce noticeable flickers in TDTN active matrix displays.

## V. CONCLUSIONS

Bond-breaking and the subsequent oxidation reactions occur in PI films during the broadband UV illumination in air. As a result, the chemical structure and surface composition of UV-modified PI films are different from the unilluminated PI. Since the surface properties, especially the surface tension and pretilt angle, of UV-modified PI films have changed, the interaction between LC and PI alignment films will also be altered. The pretilt angle decreased with the increase of the amount of UV radiation. UV illumination is thus an effective tool for surface modification of the alignment layers to achieve the desired LC alignment. This technique can be used to achieve TDTN & LC display with improved viewing angle characteristics. This method is very promising because it shows a simple route to making LC display with wider viewing angle. However, it should be noted that UV exposure not only decreases the pretilt angle

but also could affect the display performance. The change in PI charges can introduce image sticking and noticeable flickers, if dc offset voltage exceeds a certain value.

## ACKNOWLEDGMENTS

Financial support for this project was provided by the Center for Display Technology and Manufacturing at the University of Michigan. Help from Tong Li and C.S. Chiang with FTIR and  $C-V$  measurements, respectively, was greatly appreciated. The portion of this work performed at Sandia National Laboratories was supported by the U.S. Department of Energy under Contract No. DE-AC04-94AL85000.

- <sup>1</sup> K. Takatori, K. Sumiyoshi, Y. Hirai, and S. Kaneko, *Japan Display*, 1992, p. 591.
- <sup>2</sup> K. H. Yang, in *Record of the 1991 International Display and Research Conference*, San Diego, CA (IEEE, Piscataway, NJ, 1991), p. 68.
- <sup>3</sup> T. Hashimoto, T. Sugiyama, K. Katoh, T. Saitoh, H. Suzuki, Y. Limura, and S. Kobayashi, in *SID 1995 Digest*, p. 877.
- <sup>4</sup> Y. Koide, T. Kamada, K. Okamoto, M. Ohashi, I. Tomita, and M. Okabe, *SID 1992 Digest*, p. 798.
- <sup>5</sup> Y. Limura, S. Kobayashi, T. Sugiyama, Y. Toko, T. Hashimoto, and K. Kato, *SID 1994 Digest*, p. 915.
- <sup>6</sup> A. Dyadyusha, A. Khizhnyak, T. Marusii, V. Reshetnyak, Y. Reznikov, and D. Voloshchenko, *Proc. SPIE* **2408**, 151 (1995).
- <sup>7</sup> S. H. Jamal, J. R. Kelly, and J. L. West, *Jpn. J. Appl. Phys.* **1** **34**, L1368 (1995).
- <sup>8</sup> M. Hasegawa and Y. Taira, in *IRDC '94 Digest*, 1995, p. 213.
- <sup>9</sup> K. P. Ghiggino, *ACS Symp. Ser.* **381**, 27 (1989).
- <sup>10</sup> A. Lien, R. A. John, M. Angelopoulos, K. W. Lee, H. Takano, K. Tajima, A. Takenaka, K. Nagayama, Y. Momoi, and Y. Saitoh, *Asia Display '95 Digest*, p. 593.
- <sup>11</sup> J. Lu, S. V. Deshpande, J. Kanicki, A. Lien, R. A. John, and W. L. Warren, in *AMLCD '95 Digest*, p. 97.
- <sup>12</sup> T. J. Sacheffer and J. Nehring, *J. Appl. Phys.* **48**, 1783 (1977).
- <sup>13</sup> J. H. O'Donnell, *ACS Symp. Ser.* **381**, 8 (1989).
- <sup>14</sup> J. C. Coburn, M. T. Pottiger, and C. A. Pryde, *Mater. Res. Soc. Symp. Proc.* **308**, 475 (1993).
- <sup>15</sup> M. Dole, *The Radiation Chemistry of Macromolecules* (Academic, New York, 1972), Vol. 1, p. 282.
- <sup>16</sup> D. Campbell, *Polymer characterization: Physical Techniques* (Chapman and Hall, New York, 1989), Chap. 4.
- <sup>17</sup> Y. Momose, K. Ikawa, T. Sato, and S. Okazaki, *J. Appl. Polym. Sci.* **33**, 2715 (1987).
- <sup>18</sup> S. Lazare, P. D. Hoh, J. M. Baker, and R. Srinivasan, *J. Am. Ceram. Soc.* **106**, 4288 (1984).
- <sup>19</sup> H. J. Leary and D. S. Campbell, *ACS Symp. Ser.* **162**, 419 (1981).
- <sup>20</sup> K. Y. Han, P. Vetter, and T. Uchida, *Jpn. J. Appl. Phys.* **1** **32**, L1242 (1993).
- <sup>21</sup> Y. Tanaka, T. Ninomiya, M. Okamoto, N. Fkuska, and H. Hatoh, in *AMLCD '95 Digest*, p. 165.
- <sup>22</sup> T. Sasaki, M. Tsumura, Y. Nagae, M. Suzuki, and T. Iwata, *Electr. Commun. Jpn.* **78**, 79 (1995).
- <sup>23</sup> J. Cognard, *Mol. Cryst. Liq. Cryst. Suppl. Series*, **1**, 1 (1982).
- <sup>24</sup> J. G. Grabmaier, *Applications of Liquid Crystals* (Springer, New York, 1975), p. 100.
- <sup>25</sup> A. N. Seeboth, *Angew. Makromol. Chem.* **196**, 101 (1992).
- <sup>26</sup> S. Wu, *J. Adhes.* **5**, 39 (1973).
- <sup>27</sup> T. Abe and H. Fukuro, *Org. Synth. Chem. (Jpn.)* **49**, 145 (1991).
- <sup>28</sup> K. Tsuda, H. Wakemoto, and S. Ishihara, *U.S. Patent No. 5,280,375* (1994).
- <sup>29</sup> S. Kaneko, Y. Hirai, and K. Sumiyoshi, in *SID 1993 Digest*, p. 265.